(Received 30 December 2025, Accepted 20 January 2026, Scheduled 13 February 2026)

Design and Analysis of a Symmetric CPW-Fed Slot Ring Antenna with Uniform Gaps for Multi-Band ISM, WiMAX, Satellite Applications

Ravi K. Maddumala[1], Kollipara Radha[1], Udara Yedukondalu[2], Vasudha V. Bolisetty[3], and Kottapadikal V. Vineetha[4,*]

[1]*Department of Electronics and Communication Engineering Sir CR Reddy College of Engineering, Eluru, Andhra Pradesh 534007, India*
[2]*Department of ECE, MVR College of Engineering and Technology Paritala, Andhra Pradesh 521180, India*
[3]*Department of ECE, Aditya University, Surampalem 533437, India*
[4]*Department of Electronics and Communication Engineering KLEF (deemed to be University), Vaddeswaram, Guntur 522502, India*

ABSTRACT: In this study, we describe a circular ring slot antenna with three circular holes, which is supplied by a CPW-fed split ring resonator metamaterial. This proposed antenna covers sophisticated satellite communication applications for wireless devices, including 5G, military, and aerial radar, and resonates between 2.4 GHz and 10.4 GHz, with a center frequency of 3.542 GHz and an S_{11} of -37.7 dB, and a center frequency of 7.5 GHz and an S_{11} of -30.4 dB, respectively. The produced antenna satisfactorily validates the specified antenna metrics. The suggested antenna is built on an affordable FR4 substrate and has physical dimensions of $38 \times 38 \times 1.6\,\text{mm}^3$. The proposed simulated design is validated by the measured data. The results show a good correlation between the measured data and the simulation. The operational impedance range of the proposed antenna is less than -10 dB. The circular ring slot antenna has proven to be remarkably capable of reaching multiband frequencies of 3.54 GHz and 7.5 GHz. The proposed antenna may have an effect on radiation characteristics and gain, resulting in a good contender. Each component of the circle-shaped ring slot antenna design is essential to achieving the important and encouraging results.

1. INTRODUCTION

Nowadays, 5G communication antennas are one of the vital parts in wireless communication devices, since they act as a bridge between transmitter and receiver with the fast growth of today's technology. There have been huge requirements for the antennas that are small in size and good at performance. Standard antennas often face challenges of having a large size at lower frequencies, which makes them less acceptable for small wireless devices. To challenge this issue, engineers have explored new geometries and resonant contributing structures that can attain small-sized devices without degrading efficiency [1, 2].

Among these methods, split-ring resonators (SRRs) have attracted more attention for their capability to develop good resonance within a small space. The SRR's initiate inductive and capacitive effects support varying the antenna frequency to specific bands. This kind of quality makes the SRR-outlined antennas a good choice for most of the applications that need small size and good selectivity [3–5].

In [6], dual-band split-ring resonators are adopted to design two notched working bands. In [7], a Fibonacci ultra-wideband (UWB) antenna is described. The slots are incorporated in the ground plane as well as the feed line that yields triple-band characteristics. A split-ring resonator-loaded hexagon patch is designed to implement dual-notched band shown in [8]. The easiest and most effective way of improving antenna performance is to introduce slots in the radiating patch or ground plane as given in [9–12]. Ref. [13] employs a parasitic slit to create the dual-notch effect. In [14], a dumbbell-shaped slot, in both the patch and ground plane, is helpful to obtain a dual-notch structure. Similarly, a dual-band notch is notched on a pi-shaped slot-structured radiator in [15]. In [16], a T-shaped slotted antenna with an inverted 'U'-shaped slot in the feed line is presented. Ref. [17] uses an open quarter-wave stub for creating band-notch response characteristics. In [18], by loading SRR and complementary SRR (CSRR) structures, a triple notch band feature is recorded. A U-shaped slotted antenna with metamaterials is reported in [19–21].

A circular microstrip patch antenna incorporating semi-circular slits is presented in this work for Industrial, Scientific, and Medical (ISM), WiMAX, and satellite communication applications. A systematic design evolution process is carried out to validate the optimal antenna configuration and to illustrate the impact of geometrical modifications on antenna performance. The proposed antenna exhibits dual-band resonance

* Corresponding author: Kottapadikal Vinodan Vineetha (vineethaammu72@gmail.com).

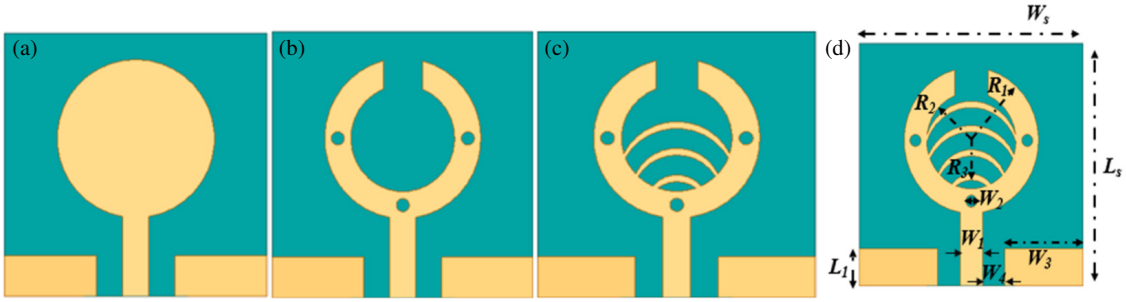

FIGURE 1. Evolvement of circular split ring resonator slotted patch in (a) Stage-1, (b) Stage-2, (c) Stage-3, (d) Stage-4.

and achieves a wide impedance bandwidth of 2.4–10.4 GHz, corresponding to an enhanced bandwidth of approximately 8 GHz. Furthermore, the radiation characteristics in both the E-plane and H-plane are analyzed at the two resonant frequencies to demonstrate stable and consistent radiation behaviour.

2. DEVICE DESIGN

The split-ring resonator-based antenna with evolution steps is discussed in Fig. 1. The stage development is featured in four stages. In Stage 1 (Fig. 1(a)), the antenna design started with a basic microstrip fed with no slits and slots on the patch. In Stage 2 (Fig. 1(b)), a circular ring-like structure is proposed having circular slots on the patch. This kind of circular hole on the patch introduces capacitance. The ring-like structure contributes more to inductance. Capacitance and inductance together develop a resonant structure later, which helps in tuning the frequency response. In Stage 3 (Fig. 1(c)), three additional split-ring resonators are added to the circular ring, which therefore increases the resonance effect. In Stage 4 (Fig. 1(d)), the final split-ring resonator is added to the circular ring, which enhances the antenna's capability to work at different operating bands. The final structure is helpful in achieving a compact size and better performance. Fig. 2 shows the dimensional details like lengths, widths, and radii, which are optimized to tune the frequency and impedance characteristics.

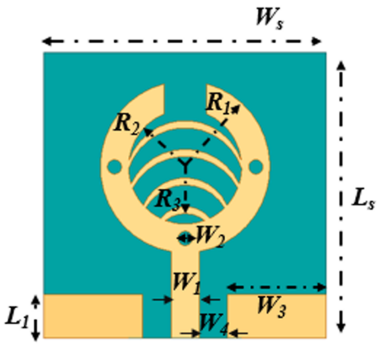

FIGURE 2. The schematic of a circular split-ring resonator antenna with CPW feed.

The circular slotted patch values with dimensions are discussed in Table 1. The impedance is tuned by adding an additional tuning branch in the RLC circuit in Fig. 3, and signal matching over a wide frequency band can be enhanced using this antenna. Such branches of Rtune, Ltune, and Ctune, however, do not contribute to yielding a strong new resonance but help balance the response from main frequency bands. The resistor Rtune serves to vary the amount of energy absorbed such that return loss is maintained, and impedance is maintained flat. The ripples or disorder between resonant peaks can be decreased by selecting an appropriate value for the resistor. That is, the antenna shows quite uniform and steady operability between such lower and upper frequencies.

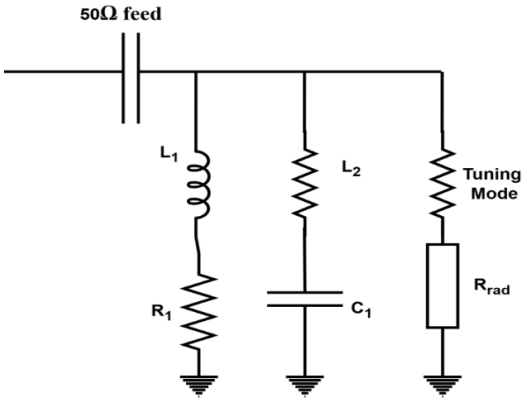

FIGURE 3. RLC circuit of circular slotted patch design.

3. RESULTS AND DISCUSSION

The optimized parameters of the design are shown in Table 1. The finite-difference time-domain (FDTD) method was employed in the optimization process to realize ultra-wideband performance. The fabricated, simulated, and measured results (Fig. 5 and Fig. 6) of the circular slotted antenna with two semi-circular rings on the ground plane are presented in this section. The S_{11} results of the reflection coefficients shown in Fig. 4 show that the antenna performs well at two resonant frequencies, which are 3.4 GHz and 10.4 GHz, with good return loss levels of -37.7 dB and -30.4 dB, respectively.

Figure 4 presents the evolution in the reflection coefficient throughout the design process. In Antenna 1 (2.51–4.2 GHz, 6.15–8.06 GHz, 8.6–9.3 GHz), the structure originates as a basic circular patch with full ground and resonates at a triple-band frequency (3.12 GHz, 7.2 GHz, 8.9 GHz) with S_{11} =

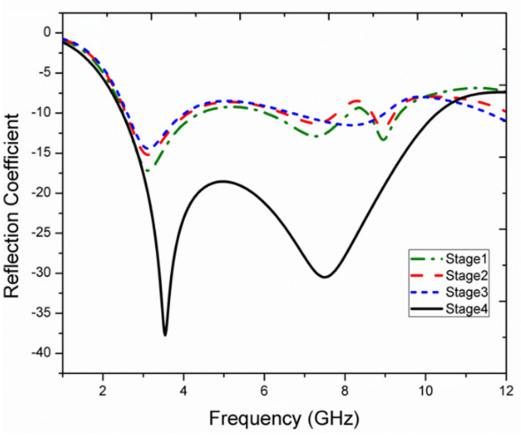

FIGURE 4. Comparison across different design stages of the semicircular slotted patch.

TABLE 1. Circular slotted patch values with dimension.

Value	Dimension (mm)	Value	Dimension (mm)
L_s	38	W_3	16
W_s	38	W_4	2
L_1	4	R_1	8
W_1	2	R_2	6
W_2	0.7	R_3	5.5

$(-17.1\,\text{dB}, -12.8\,\text{dB}, -13.3\,\text{dB})$. The impedance bandwidth is less than $-10\,\text{dB}$.

In Antenna 2 (2.5–4.1 GHz, 6.5–7.7 GHz, 8.6–9.1 GHz), one semicircular ring slot on the patch and one hexagonal cut in the ground are included. This change creates three resonant points (3.1 GHz, 7.2 GHz, and 8.9 GHz), ($-15.2\,\text{dB}$, $-11.2\,\text{dB}$, and $-11.9\,\text{dB}$), but the bandwidth enhancement is still confined. In Antenna 3 (2.6–3.95 GHz, 6.9–8.9 GHz), three half-wavelength ring slots are incorporated on the patch to achieve good resonance characteristics and frequency tuning. This change creates two resonant points (3.1 GHz, 8.1 GHz), and its reflection coefficients will be shifted to ($-14.4\,\text{dB}$, $-11.5\,\text{dB}$).

At last, three round slots are printed on the main circular ring of Antenna 4 (2.4 GHz–10.4 GHz), and four semicircular slots are made up in the patch. This last version provides ultra-wideband operation from 2.4 GHz to 10.4 GHz, center frequencies at 3.4 GHz and 10.4 GHz, and very good return losses of $-37.7\,\text{dB}$ and $-30.4\,\text{dB}$, respectively.

Figure 5(a) establishes how slot width (W_1) influences the antenna reflection features. When W_1 varies from 0.5 mm to 0.7 mm, the resonant peaks are shifted, and the frequency ranges of dips change with depth as well. A long narrow slot is further used to stabilize the resonance, and a short wide slot is for controlling coupling and frequency shift tuning. This happens due to larger slots that affect the E field around the patch. Out of the three, $W_1 = 0.7$ mm is a good choice in terms of resonance and return loss. It is shown in this deposition that the width of the slot value affects the impedance and contributes to achieving a good frequency tuning.

Figure 5(b) demonstrates that varying the (R_1) of the semicircular slot influences the performance of the antenna. When the radius changes from 7.8 mm to 8.0 mm, the major resonant position slightly shifts to a lower frequency. It is because a larger radius, which allows the traveling path for the surface current to be longer, causes a decrease in operating frequency. The minimum at 3.5 GHz is indicative of an efficient radiation with good matching. Small modifications even cause the effective frequency range of the higher bands to be shifted a little bit. For the curve with $R_1 = 7.9$ mm, the response is enhanced, which reveals that the antenna has good tuning and stable bandwidth.

The developed prototype structure is depicted in Fig. 6, and Fig. 7 shows the measured and simulated S_{11} values, respectively. The good agreements between the two results demonstrate that the antenna design is reliable.

This plot shows how the antenna improves through design stages. In the first stage, only one resonance appears with a minimum bandwidth. The number of operating points increases, and the return loss becomes smaller as more extra slots or structural variations are added in the next stages. At Stage 4, the antenna has wideband performance and good matching with many bands. Every update improves the current path and enhances energy coupling. This progressive development demonstrates how the design matures to a better and broadband antenna through successive optimization. Fig. 7 shows a graph (simulated and measured) for the reflection coefficients of the last antenna. The two curves have a similar tendency and display two well-defined peak bands around 3.5 GHz, and 8.5 GHz, respectively. The good agreement between simulation and measurement proves that the fabricated antenna operates as it was designed. Small discrepancies between the two antennas might arise from soldering.

The radiation plot shows how the antenna emanates energy in both the planes at two different operating frequencies, i.e., 3.5 GHz and 10.4 GHz. Here, the E-plane indicates electric fields, and the H-plane indicates magnetic field distributions. At 3.5 GHz, radiation patterns are almost similar; they present stable radiation. E-fields demonstrate stronger radiation in the main orientation, while the H-plane maintains a balanced uniform spread. At 10.4 GHz, both planes show directional patterns, indicating that the design is more concentrated at high frequencies. The close match between simulated and practical patterns is accurately good in practical conditions, maintaining better consistent and stable patterns in Fig. 8.

The suggested antenna's three-dimensional radiation patterns at two operating frequencies are displayed in Fig. 9. (a) The antenna shows a wide and steady radiation pattern at 3.4 GHz, with the boresight receiving the most radiation, suggesting strong coverage appropriate for WLAN/IoT applications. (b) At 10.4 GHz, a more directive radiation pattern is observed with a somewhat smaller beamwidth.

These graphs of electric and magnetic fields show how energy flows — and radiates off the surface of the antenna (Fig. 10), where E-field is the electric strength, and it is mainly distributed around the circular edges, slots, and feed point. These regions indicate where charge can build up, and voltage

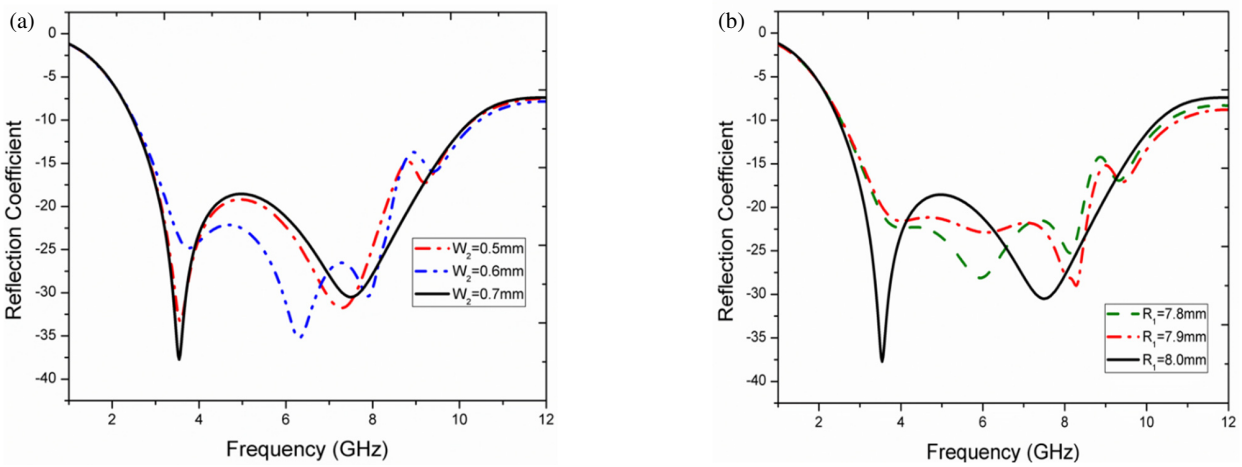

FIGURE 5. S_{11} response for different (a) (W_2) values of the semicircular slotted patch, influences the resonance position and bandwidth. Variation of S_{11} with different, (b) (R_1) values of the semicircular slotted patch, resonant frequency, and impedance matching.

TABLE 2. Comparison of the proposed circular slotted with previously reported designs, highlighting improvements.

Ref.	Dimension (mm^3)	Centre frequency (GHz)	Bandwidth (MHz)	Gain (dBi)	Application
[5]	$53 \times 38.5 \times 1.6$	2.44 5.25	2.1	4.85	UWB
[7]	$55 \times 54 \times 1.59$	3.3–3.6 5.15–5.35 5.93–7.15	300 200 1220	6	WiMax, LTE band
[15]	$52 \times 40 \times 0.62$	3.3–3.7 6.5–7.2	400 700	6	WiFi WLAN
[19]	$55 \times 54 \times 1.59$	3.3–3.6	300	6	WiMAX, IOT
This work	$38 \times 38 \times 1.6$	2.4–10.4 3.4 10.4	8000	6.98 6.31	ISM WiMAX Satellite communication

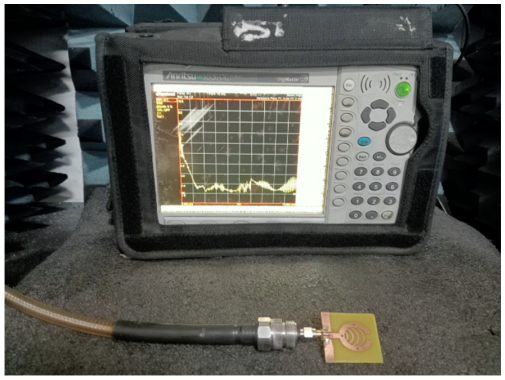

FIGURE 6. Fabricated prototype of the circular slotted antenna.

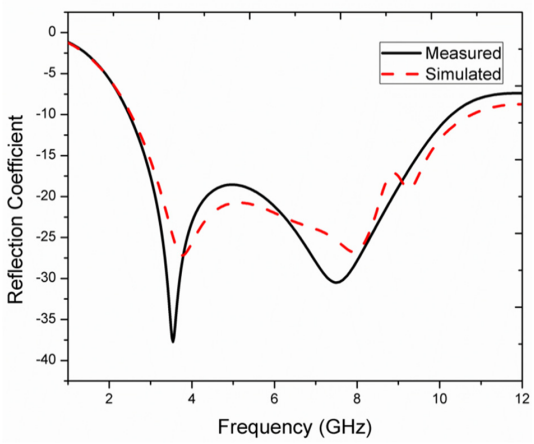

FIGURE 7. Comparison between simulated and measured S_{11} of the designed antenna.

changes take place, which causes the antenna to efficiently radiate signals. With increasing frequency, the E-field is widened towards the edges of the arcs, demonstrating that they are paths for current and depend on frequency. The H-field is the magnetic intensity due to surface currents. It is most intense near the feed and along the curved slots, where most of the current flows. This magnetic activity helps the radiation field and ac-

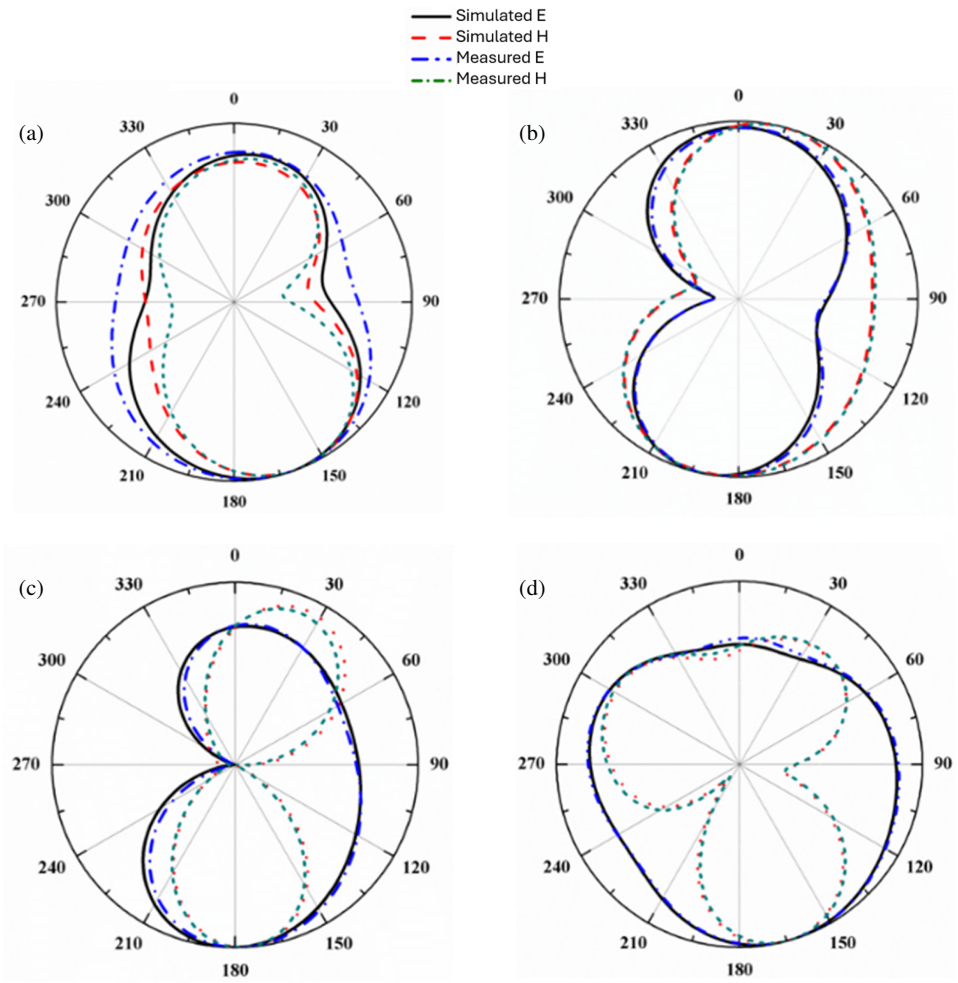

FIGURE 8. The simulated and measured pattern characteristics of the antenna at XY plane, (a) 3.5 GHz, (b) 10.4 GHz XZ plane, (c) 3.5 GHz, (d) 10.4 GHz frequencies respectively.

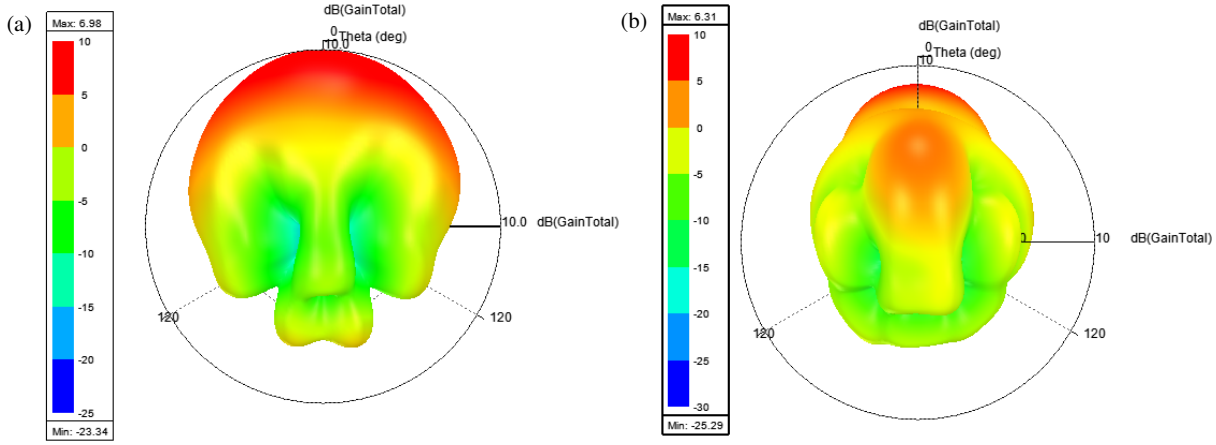

FIGURE 9. Three-dimensional polar graphs circular split slotted patch design.

celerates energy transfer. Take the E-field and H-field in combination; the E-field-H-field patterns indicate both electric and magnetic resonances involved in the antenna to obtain good radiation properties and a wide operating bandwidth.

The simulated return loss (S_{11}) of the suggested antenna, as determined by ANSYS High Frequency Structure Simulator (HFSS) and Advanced Design System (ADS) software, is depicted in the image. At around 3.54 GHz and 7.5 GHz, two distinct resonant modes are seen, with profound impedance

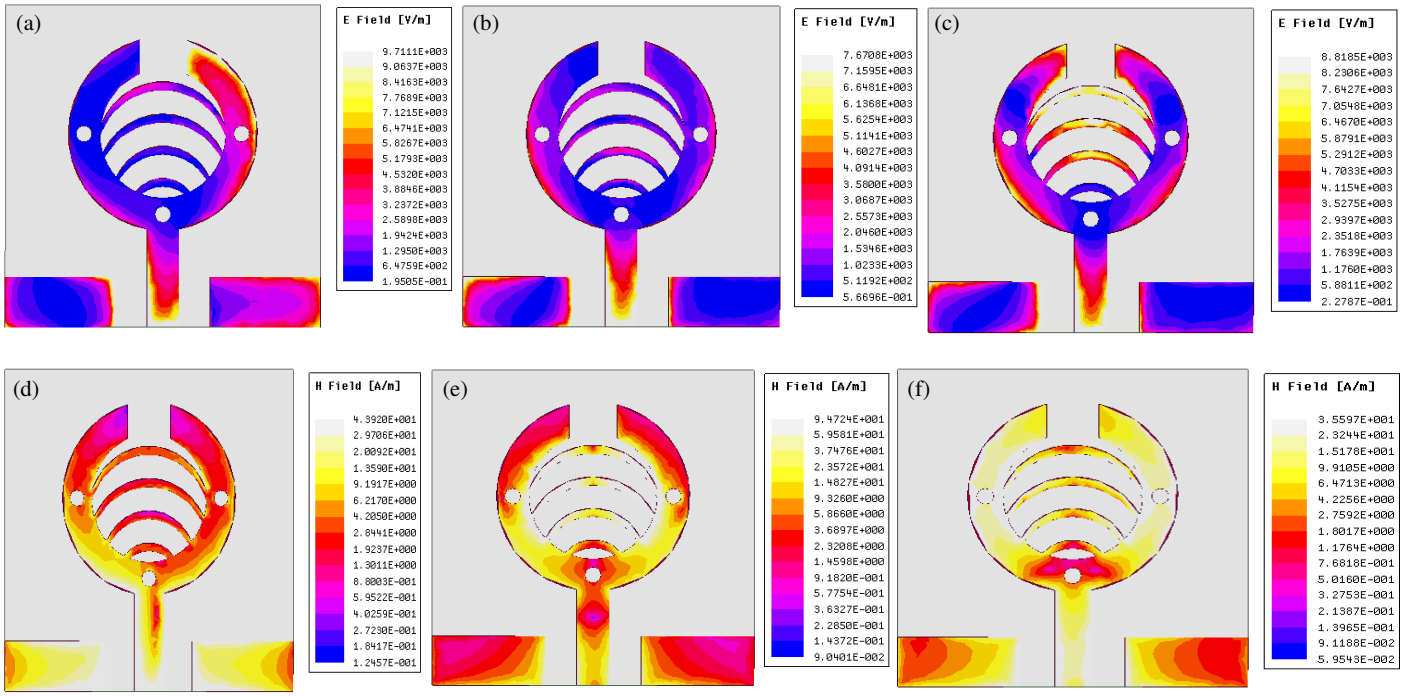

FIGURE 10. Surface current distribution (Stage 4) at 3.54 GHz and 7.57 GHz, demonstrating the electric (E-field) and magnetic (H-field) across the surface.

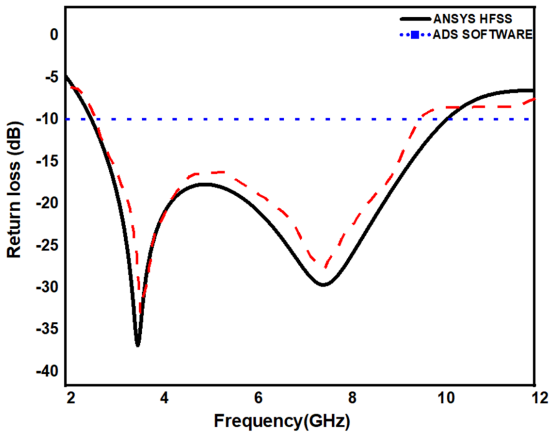

FIGURE 11. Return loss value of the proposed antenna with ANSYS HFSS and ADS software.

matching reaching approximately −37 dB and −30 dB, respectively. The antenna confirms wideband multiband functioning by keeping S_{11} below −10 dB between 2.4 GHz and 10.4 GHz. The close agreement between the two solvers' findings confirms the design's dependability. Variations in meshing methods and numerical solvers are the cause of small discrepancies between curves in Fig. 11. All things considered, the outcomes show outstanding impedance matching appropriate for multiband wireless applications.

The suggested antenna is contrasted with current designs described in [5, 7, 15, 19] in Table 2. The antennas in [5, 7, 15] have restricted operational ranges and application coverage, while achieving narrow or segmented bandwidths (300–1220 MHz) with modest gain. UWB performance is provided by the design in [19], although at the expense of greater structural complexity and bulk. The suggested antenna, on the other hand, has a substantially larger impedance bandwidth of 2.4–10.4 GHz (8 GHz) and competitive gain of up to 6.98 dBi in a small $38 \times 38 \times 1.6\,\text{mm}^3$ footprint. Wider applications, such as ISM, WiMAX, and satellite communication, are made possible by this excellent bandwidth-size-gain trade-off.

4. CONCLUSION

In conclusion, the coplanar waveguide (CPW)-fed circular ring slot antenna with equal gaps of this particular design exhibits excellent performance over numerous frequency bands. The use of both split-ring resonators and circular holes has yielded antennas with increased bandwidth and matched impedances. As a consequence, it can be used efficiently in the frequency range of 2.4 GHz and 10.4 GHz. The designed antenna has several applications: ISM, WiMAX, fifth-generation wireless communication systems, and the military and satellite broadcast. It has been analyzed that the measured data and the simulation results agree, so the design is correct as well. The additional RLC tuning branch to the loop helps to overcome the impedance to variations outside of the resonance by stabilizing outside frequency response. With a compact size of $38 \times 38 \times 1.6\,\text{mm}^3$ on an FR4 dielectric substrate at a frequency of 2.4 GHz. This antenna is an excellent balance between performance and price. In summary, the design of this antenna is very stable through a compact size and very helpful for end devices in wireless communication equipment nowadays.

REFERENCES

[1] Hossain, M. J., M. R. I. Faruque, and M. T. Islam, "Design of a patch antenna for ultra wide band applications," *Microwave and Optical Technology Letters*, Vol. 58, No. 9, 2152–2156, 2016.

[2] Saha, T. K., C. Goodbody, T. Karacolak, and P. K. Sekhar, "A compact monopole antenna for ultra-wideband applications," *Microwave and Optical Technology Letters*, Vol. 61, No. 1, 182–186, 2019.

[3] Kadam, A. A., A. A. Deshmukh, S. B. Deshmukh, A. Doshi, and K. P. Ray, "Slit loaded circular ultra wideband antenna for band notch characteristics," in *2019 National Conference on Communications (NCC)*, 1–6, Bangalore, India, 2019.

[4] Khandelwal, M. K., B. K. Kanaujia, and S. Kumar, "Defected ground structure: Fundamentals, analysis, and applications in modern wireless trends," *International Journal of Antennas and Propagation*, Vol. 2017, No. 1, 2018527, 2017.

[5] Prakash, K. C., S. Mathew, R. Anitha, P. V. Vinesh, M. Jayakrishnan, P. Mohanan, and K. Vasudevan, "Circularly polarized dodecagonal patch antenna with polygonal slot for RFID applications," *Progress In Electromagnetics Research C*, Vol. 61, 9–15, 2016.

[6] Abu Safia, O., M. Nedil, L. Talbi, and K. Hettak, "Coplanar waveguide-fed rose-curve shape UWB monopole antenna with dual-notch characteristics," *IET Microwaves, Antennas & Propagation*, Vol. 12, No. 7, 1112–1119, 2018.

[7] Srivastava, K., A. Kumar, B. K. Kanaujia, S. Dwari, A. K. Verma, K. P. Esselle, and R. Mittra, "Integrated GSM-UWB Fibonacci-type antennas with single, dual, and triple notched bands," *IET Microwaves, Antennas & Propagation*, Vol. 12, No. 6, 1004–1012, 2018.

[8] Zeng, Y., H. Zhang, Y. Zhang, and H. Zhao, "Compact band-notched UWB antenna based on CSRR for WiMAX/WLAN applications," in *2018 International Conference on Microwave and Millimeter Wave Technology (ICMMT)*, 1–3, Chengdu, China, 2018.

[9] De, A., B. Roy, and A. K. Bhattacharjee, "Dual-notched monopole antenna using DGS for WLAN and Wi-MAX applications," *Journal of Circuits, Systems and Computers*, Vol. 28, No. 11, 1950189, 2019.

[10] Seo, Y. S., J. W. Jung, H. J. Lee, and Y. S. Lim, "Design of trapezoid monopole antenna with band-notched performance for UWB," *Electronics Letters*, Vol. 48, No. 12, 673–674, 2012.

[11] Bhattacharya, A., B. Roy, S. K. Chowdhury, and A. K. Bhattacharjee, "Compact slotted UWB monopole antenna with tuneable band-notch characteristics," *Microwave and Optical Technology Letters*, Vol. 59, No. 9, 2358–2365, 2017.

[12] Sharma, P., K. Vyas, and R. P. Yadav, "Design and analysis of miniaturized UWB antenna with tunable notched band," *International Journal of Microwave and Wireless Technologies*, Vol. 9, No. 3, 691–696, 2017.

[13] Ye, L.-H. and Q.-X. Chu, "3.5/5.5 GHz dual band-notch ultra-wideband slot antenna with compact size," *Electronics Letters*, Vol. 46, No. 5, 325–327, 2010.

[14] Salamin, M. A., W. Ali, and A. Zugari, "Design and analysis of a miniaturized band-notched planar antenna incorporating a joint DMS and DGS band-rejection technique for UWB applications," *Microsystem Technologies*, Vol. 25, No. 9, 3375–3385, 2019.

[15] Peddakrishna, S. and T. Khan, "Design of UWB monopole antenna with dual notched band characteristics by using π-shaped slot and EBG resonator," *AEU — International Journal of Electronics and Communications*, Vol. 96, 107–112, 2018.

[16] Mukherjee, B., S. G. Thakurta, R. Roy, A. Das, A. Banerjee, I. Aich, S. Mukherjee, and A. Mukherjee, "Coplanar waveguide fed ultra-wide band printed slot antenna with dual band-notch characteristics," in *2017 8th Annual Industrial Automation and Electromechanical Engineering Conference (IEMECON)*, 314–317, Bangkok, Thailand, 2017.

[17] Lui, W. J., C. H. Cheng, and H. B. Zhu, "Frequency notched printed slot antenna with parasitic open-circuit stub," *Electronics Letters*, Vol. 41, No. 20, 1094–1095, 2005.

[18] Yadav, A., S. Agrawal, and R. P. Yadav, "SRR and S-shape slot loaded triple band notched UWB antenna," *AEU — International Journal of Electronics and Communications*, Vol. 79, 192–198, 2017.

[19] Zhou, Y., J. Huang, W. Wu, and N. Yuan, "An antipodal Vivaldi antenna with band-notched characteristics for ultra-wideband applications," *AEU — International Journal of Electronics and Communications*, Vol. 76, 152–157, 2017.

[20] Ansari, J., N. P. Yadav, P. Singh, and A. Mishra, "Compact half U-slot loaded shorted rectangular patch antenna for broadband operation," *Progress In Electromagnetics Research M*, Vol. 9, 215–226, 2009.

[21] Bonache, J., M. Gil, I. Gil, J. Garcia-Garcia, and F. Martin, "On the electrical characteristics of complementary metamaterial resonators," *IEEE Microwave and Wireless Components Letters*, Vol. 16, No. 10, 543–545, 2006.